The J = 2 ortho levels of the v = 0 to 6 np singlet Rydberg series of molecular hydrogen revisited

M. Glass-Maujean, H. Schmoranzer, I. Haar, A. Knie, P. Reiss, and A. Ehresmann

Citation: The Journal of Chemical Physics **137**, 084303 (2012); doi: 10.1063/1.4742311
View online: http://dx.doi.org/10.1063/1.4742311
View Table of Contents: http://scitation.aip.org/content/aip/journal/jcp/137/8?ver=pdfcov
Published by the AIP Publishing

The $J = 2$ ortho levels of the $v = 0$ to 6 np singlet Rydberg series of molecular hydrogen revisited

M. Glass-Maujean,[1] H. Schmoranzer,[2] I. Haar,[3] A. Knie,[3] P. Reiss,[3] and A. Ehresmann[3]
[1]*Laboratoire de Physique Moléculaire pour l'Atmosphère et l'Astrophysique, UMR 7092 UPMC/CNRS, Université Pierre et Marie Curie, 4 place Jussieu, 75252 Paris Cedex 05, France*
[2]*Fachbereich Physik, Technische Universität Kaiserslautern, D-67653 Kaiserslautern, Germany*
[3]*Institute of Physics and Interdisciplinary Nanostructure Science and Technology, Heinrich-Plett-Str. 40 Universität Kassel, D-34132 Kassel, Germany*

(Received 14 June 2012; accepted 20 July 2012; published online 23 August 2012)

The energies of the $J = 2$ ortho levels of the $v = 0$ to 6 Rydberg np singlet series of molecular hydrogen with absolute intensities of the R(1) and P(3) absorption lines were measured by a high-resolution synchrotron radiation experiment and calculated through a full *ab initio* multi-channel quantum defect approach. © *2012 American Institute of Physics*. [http://dx.doi.org/10.1063/1.4742311]

I. INTRODUCTION

This paper continues a series within the framework of a joint experimental and theoretical systematic study of the absorption spectrum of molecular hydrogen.[1–5] In the first papers[1–3] we investigated the manifold of excited singlet *ungerade* J levels corresponding to $J \geq 1$ and total parity $-(-1)^J$. These levels have pure $^1\prod_u^-$ electronic symmetry and are not subject to rotational-electronic non-adiabatic couplings (to a very good approximation). We presented then the $J = 0$ levels,[4] which have pure $^1\sum_u^+$ electronic symmetry; they are not influenced by rotational-electronic non-adiabatic couplings either. In the last paper we investigated the $J = 1$ para levels. They have either $^1\sum_u^+$ or $^1\prod_u^+$ electronic symmetry in the Born-Oppenheimer approximation and are slightly mixed by rotational interaction. Here we are concerned with the $J = 2$ ortho levels. They also have either $^1\sum_u^+$ or $^1\prod_u^+$ electronic symmetry in the Born-Oppenheimer approximation and the rotational interaction, increasing as the product $J(J + 1)$, is more efficient. They can be populated by the R(1) absorption lines which are, with the Q(1) lines (with $^1\prod_u^-$ $J = 1$ upper levels), the most intensive lines of the spectrum.

These levels had been studied experimentally from $v = 0$ to $v = 3$ in a pioneering work already forty years ago.[6] The measured energies, obtained on a photographic plate, had an uncertainty of 0.3 cm^{-1} only in most cases. The line intensities, however, have not been measured. Few years later, the photoionization spectrum of H_2, at low temperature, was recorded and the R(0) lines were tabulated with their intensities for $v = 0$ to 6; the R(1) lines, however, were assigned on the spectrum figures only.[7] In that work, the uncertainty of the energy measurement was about 4.5 cm^{-1}. Later on, the autoionization of the R(1) lines was studied by a double resonance experiment to investigate the vibrational branching ratios of the fragments of the $v = 2$ series[8] and the rotational distribution of the $v = 1$ series.[9] The assignments of several lines were then revisited.

Theoretically, the levels of molecular hydrogen have been used extensively as bench marks for the improvement of the various theoretical approaches, but except for the first multi-channel quantum defect (MQDT) attempt[6] there are no systematic calculations of the level energies and there are nearly no calculations of the line intensities before our own work.[1–5]

Since the hydrogen nuclei are only 1836 times heavier than the electrons and the classical frequency of electronic motion becomes progressively slower as the energy increases along a Rydberg series, the electronic motion may occur on the same time scale as vibration or rotation and energy transfer between the electron and the nuclei is possible. In order to reproduce theoretically these transfers, quantum chemistry first describes the energies of the electronic states at fixed positions of the nuclei, then evaluates the adiabatic corrections which are due to the diagonal terms of the Hamiltonian part depending on the velocity of the nuclei, and then calculates the non-diagonal terms. For the H_2 molecule, which is the simplest one and the most amenable to *ab initio* calculations, these coupling functions have been calculated for the 10 first electronic states: the 6 first $^1\sum_u^+$ states and the 4 first $^1\prod_u$ states.[10] The energies of the rovibronic levels of these states have been calculated provided the levels are not predissociated. The np Rydberg states with $n > 4$ cannot be calculated with high precision by such a way. The MQDT approach is adapted to this task; in this approach, following Fano,[11] the molecular wave function is not partitioned any longer into electronic, vibrational, and rotational parts. The electron movement is described differently as a function of its distance from the core. At short distance the electron is fast, much faster than the nuclei, and the Born-Oppenheimer approximation can be considered as valid and the molecular wave function is simply expressed in the molecular frame; far from the core, the electron experiences the electric field of the ion and the wave function is a Coulombian solution in the laboratory frame. A frame transformation is then needed with a condition of continuity. The most striking advantage of MQDT is that it entirely eliminates the usual laborious steps of evaluating the interactions between a large number of neighboring and distant electronic states in terms of off-diagonal rovibronic matrix elements derived from the Hamiltonian. Instead, the various terms of the Hamiltonian coupling

the Rydberg electron to the core are replaced by their net effect on its radial function outside the core. For a bound electron this effect is embodied in the quantum defect μ. By focusing the attention on the radial function *outside* the core, MQDT replaces the concept of individual interacting *molecular states* by that of interacting *channels*, each channel being defined by the orbital quantum number l of the emerging electron and by a particular rovibronic state of the residual core.[12–20]

We performed a MQDT calculation similar to those of the above references, but the quantum defects, which are the only data needed, were extracted from highly accurate *ab initio* clamped-nuclei (Born-Oppenheimer) potential energy curves;[21,22] these quantum defect functions were previously presented in Refs. 1 and 4. The calculations are then fully *ab initio*. The MQDT approach can be used to calculate also the line intensities.[19] Even a small non-adiabatic mixing, quite ineffective on the energies of the levels, influences visibly the intensities of the lines,[1–3] so that the line intensity calculations provide a very sensitive test and proof of the non-adiabatic couplings.

Together with these *ab initio* calculations, we present here not only the measurements of the level energies (with an uncertainty of 1 cm^{-1}), but also of the line intensities (in absolute units) which constitute an important tool to interpret the spectra.

Due to technical difficulties in the calculations of the predissociated levels in this simple approach, we focused this study on the Rydberg levels with $n > 7$ which are practically unaffected by the predissociation; their dissociation yields are nearly 0% and thus below our experimental sensitivity.

II. EXPERIMENT

The experimental setup has been described in detail in previous publications.[23–26] The intensities of the absorption spectrum, recorded at high spectral resolution, have been calibrated directly, based on the known gas pressure and absorption path length. Simultaneously, the photoionization and photodissociation excitation spectra were recorded and calibrated. The vacuum ultraviolet photons coming from the undulator beamline U125/2-10m-NIM of BESSY II were dispersed by a 10 m-normal-incidence monochromator equipped with a 4800-lines/mm grating giving a spectral resolution of 0.0010 nm in first order[27] (this value represents the convolution of the apparatus function with the Doppler width at room temperature). The uncertainty of the energies of the measured spectra has been improved significantly since the previous publications[23–26] and is now about ± 1.0 cm^{-1}.

III. THEORETICAL APPROACH

A. One-level energies

The theoretical multichannel quantum defect approach used here has been discussed in numerous previous publications[12,17,19,20] and in particular in our preceding papers.[1–5] Briefly, we use quantum defect theory in a simple form by disregarding channel interactions between singly excited and doubly (core) excited Rydberg channels. This means that we assume that the manifold of $^1\sum_u^+$ and $^1\prod_u^+$ excited states of H_2 represents an isolated system of states interacting with each other but not with the others converging to the $X\ ^2\sum_g^+$ ground state of H_2^+, disregarding the couplings with the nf Rydberg series converging to the ground state of H_2^+ and the Rydberg series converging to the excited states of the ion. Correlations between the excited electron and the ion core electron are included in an effective manner in the quantum defects, because we extract the latter from highly accurate theoretical clamped-nuclei (Born-Oppenheimer) potential energy curves[21,22] in which electron correlation has been fully accounted for.

The non-adiabatic term $-(\frac{m}{8\mu})\nabla_1^2$ (finite mass correction for the outer electron) yields a mass-dependent and R-dependent correction to the clamped-nuclei quantum defect

$$\Delta\mu = -\frac{1}{4\pi} R \frac{\partial \mu}{\partial R}, \tag{1}$$

which is included; it plays a role primarily at large internuclear distances.

Specifically, we derive R- and energy-dependent quantum defects from the potential energy curves, calculated by Wolniewicz and his group,[21,22] by using the familiar Rydberg equation. The quantum defects for $^1\Sigma_u^+$ symmetry have been extracted from the curves corresponding to $n = 3$, 4, and 5 (see Ref. 4 for the details) and the quantum defects $\mu_{np\pi}$ for the $^1\Pi_u$ symmetry were extracted from the curves corresponding to $n = 2$, 3, and 4 (see Ref. 1 for the details). Due to their dependence on the principal quantum number n, these quantum defect functions depend on the energy as well as on the internuclear distance. Following the MQDT implemented in Refs. 1 and 4 they were reduced to the form of an energy- and R-dependent polynomial. These E-dependent quantum defects are used to calculate the E-dependent reaction matrix $\boldsymbol{k}(E)$.

Standard MQDT procedures[17] match the short-range electron wave function implied by the reaction matrix $\boldsymbol{k}(E)$ for a given total energy to phase-shifted electron Coulomb waves. Whereas at short internuclear distance, the molecule is well described by Hund's case b, i.e., in the molecular frame, at large distance the electron in the field of the ion, corresponding to Hund's case d described in the laboratory frame. The frame transformation has to be taken into account and the reaction matrix has to be written in the Hund's case d basis set[5,12] for a given N (for the singlet levels, $J = N$),

$$K^{(N)}_{v^+N^+=N-1,v^{+\prime}N^{+\prime}=N-1}(E) = \frac{N}{2N+1} k^{(\lambda=0)}_{v^+N^+=N-1,v^{+\prime}N^{+\prime}=N-1} + \frac{N+1}{2N+1} k^{(\lambda=1)}_{v^+N^+=N-1,v^{+\prime}N^{+\prime}=N-1}, \tag{2a}$$

$$K^{(N)}_{v^+N^+=N+1,v^{+\prime}N^{+\prime}=N+1}(E) = \frac{N+1}{2N+1} k^{(\lambda=0)}_{v^+N^+=N+1,v^{+\prime}N^{+\prime}=N+1} + \frac{N}{2N+1} k^{(\lambda=1)}_{v^+N^+=N+1,v^{+\prime}N^{+\prime}=N+1}, \tag{2b}$$

$$K^{(N)}_{v^+N^+=N-1,v^{+\prime}N^{+\prime}=N+1}(E) = -\frac{\sqrt{N(N+1)}}{2N+1} \times (k^{(\lambda=0)}_{v^+N^+=N-1,v^{+\prime}N^{+\prime}=N+1} - k^{(\lambda=1)}_{v^+N^+=N-1,v^{+\prime}N^{+\prime}=N+1}), \quad (2c)$$

$$K^{(N)}_{v^+N^+=N-1,v^{+\prime}N^{+\prime}=N+1}(E) = K^{(N)}_{v^{+\prime}N^{+\prime}=N+1,v^+N^+=N-1}(E), \quad (2d)$$

where $\lambda = 0$ for a $^1\sum^+_u$ state and 1 for a $^1\prod^+_u$ one.

Following what we did in Refs. 1–5 to match the short-range electron wave function to phase-shifted electron Coulomb waves with asymptotically correct behavior, we used the boundary condition

$$\det|\cos\beta(E)\boldsymbol{S} + \sin\beta(E)\boldsymbol{C}| = 0, \quad (3)$$

where $\mathbf{K} = \mathbf{SC}^{-1}$ and $\beta(E)$ is an asymptotic phase vector whose components $\beta_{v+}(E)$ take different values depending on whether a given v^+N^+ Rydberg channel is closed ($E < E_{v^+N^+}$) or open ($E > E_{v^+N^+}$).

For closed channels $\beta_{v^+N^+}(E) = \pi\nu_{v^+N^+}$, where $\nu_{v^+N^+}$ is the effective principal quantum number corresponding to that closed channel, related to the energy through the Rydberg rule,[12]

$$(E - E_{v^+N^+})/hc = -\frac{Ry_{H_2}}{\nu_{v^+N^+}}. \quad (4)$$

To determine the energies of the bound levels, we restricted the basis set to closed channels only.

B. Line intensities

As described previously,[4] an analogous procedure was applied to the clamped-nuclei transition dipole moment functions $d_{np\sigma}(R)$ and $d_{np\pi}(R)$ from Refs. 22 and 28 to obtain transition moment functions $d_\lambda(\varepsilon, R)$ and E-dependent transition matrix elements $d^{(\sigma,q,N)}_{v^+N^+vN}$ involving the vibrational ground state levels.

The effective transition moment from the ground state to a bound λ Rydberg level n is given by the following superposition of channel amplitudes:

$$D^\sigma_n = \frac{1}{\mathrm{N}}\sum_{v^+}\left[\sqrt{\frac{N}{2N+1}}d^{(\sigma,q,N)}_{v^+N^+=N-1,v''N''}B_{v^+N^+=N-1}(E_n) - \sqrt{\frac{N+1}{2N+1}}d^{(\sigma,q,N)}_{v^+N^+=N+1,v''N''}B_{v^+N^+=N+1}(E_n)\right] \quad (5a)$$

and

$$D^\pi_n = \frac{1}{\mathrm{N}}\sum_{v^+}\left[\sqrt{\frac{N+1}{2N+1}}d^{(\pi,q,N)}_{v^+N^+=N-1,v''N''}B_{v^+N^+=N-1}(E_n) + \sqrt{\frac{N}{2N+1}}d^{(\pi,q,N)}_{v^+N^+=N+1,v''N''}B_{v^+N^+=N+1}(E_n)\right], \quad (5b)$$

where $B_{v^+N^+}$ are the channel mixing coefficients obtained by solving Eq. (3) (on the Hund's coupling case d basis set). N is the overall normalization factor of the bound state wave function; see, e.g., Ref. 1 for detailed discussion and expressions. The rotational couplings mix the σ and π states modifying the intensities of the R and P lines to the n upper level of total angular momentum quantum number $J = N$ according to

$$A(R) = \frac{4}{3}\frac{mc^2}{\hbar}\alpha^5\left[\sqrt{\frac{N}{2N+1}}\frac{D^\sigma_n}{a_0} - \sqrt{\frac{N+1}{2N+1}}\frac{D^\pi_n}{a_0}\right]^2 \times \left(\frac{E_n - E_{v''N''}}{2hcRy}\right)^3 \quad (6)$$

for a R($N-1$) line,[29–31] and

$$A(P) = \frac{4}{3}\frac{mc^2}{\hbar}\alpha^5\left[\sqrt{\frac{N+1}{2N+1}}\frac{D^\sigma_n}{a_0} + \sqrt{\frac{N}{2N+1}}\frac{D^\pi_n}{a_0}\right]^2 \times \left(\frac{E_n - E_{v''N''}}{2hcRy}\right)^3 \quad (7)$$

for a P($N+1$) line. Here α is the fine-structure constant. The transition energy is in joules and the transition moment in meters. The ratios in (...) and in [...] correspond, respectively, to the transition energy and to the dipole moment in atomic units.

C. Numerical details

The vibration-rotation wave functions $\chi_{v^+N^+}$ were evaluated in the adiabatic approximation using the ion ground state potential energy curve of Wind[32] and the adiabatic correction terms of Bishop and Wetmore.[33] The corresponding ion levels $E_{v^+N^+}$ are those of Wolniewicz and Orlikowski,[34] calculated including the non-adiabatic and relativistic interactions in addition to the adiabatic corrections. The H_2 ground state vibrational wave function $\chi_{v''N''}(R)$ was evaluated using the potential energy curve of Wolniewicz[35] (with adiabatic corrections). The ground state energy levels were evaluated from the best determination of the ionization energy X $^1\sum^+_g$ $v'' = 0$, $J'' = 0 \rightarrow$ X $^2\sum^+_g$ $v^+ = 0$ $J^+ = 0$ and the dissociation energy of the ion.[36] The calculations were performed for various values of the maximum internuclear distance from 7 to 40 a.u. and the vibrational basis set was varied from 20 × 2 to 50 × 2. For the levels with $n > 7$, the calculated energies remained unaffected to within ~0.1 cm^{-1} or less and the line intensities to within 5%. For the lower Rydberg levels, the coupling to the dissociation continuum may be important. In the calculation, the continua are discretized and, depending on the position of the quasi continuum levels, the resonances of Rydberg levels may be shifted. This effect is important for the dissociated levels (mainly the 3pπ $^1\prod^+_u$ and 4pσ $^1\sum^+_u$ levels) and for the levels that are coupled to them. Therefore, we restricted here our investigation to the $n > 7$ levels. The full treatment will be the aim of another study.

IV. RESULTS

The energies of the $N = 2$ ortho singlet np levels of H_2 were calculated from 120 000 to 134 000 cm^{-1} with the intensities of the R(1) and P(3) absorption lines from the ground state with $v'' = 0$ to these levels. The assignments of the calculated resonances are those of the dominant part of the complex wave function. In the case of mega-resonances, the same

TABLE I. Reassigned R(1) lines. First column: calculated transition energies, this work; second column: experimental transition energies, present values in bold type. Third columns: new assignments. Forth column: formerly measured energies (Ref. 6) for the assignments in column 3. Last columns: new assignments for the formerly measured energies (Ref. 6).

Calculated energy (cm^{-1})	Exp. energy (cm^{-1})	Reassignment		v	Exp. energy from Ref. 6	New name		v
124108.58	**124108.7**	R(1)	21p1	0	124113.10	R(0)	4pπ	3
124211.53	**124211.8**	R(1)	16p3	0	124215.70	P(1)	28pσ	0
125416.24	**125416.0**	R(1)	9pπ	1	125421.50	R(0)	6pσ	2
126234.47	tw[a]	R(1)	19p1	1	126237.30	P(1)	19pσ	1
126354.58	126354.85[b]	R(1)	24p1	1	126352.10	P(1)	24pσ	1
127438.88	tw[a]	R(1)	9pπ	2	127431.60	P(1)	10pσ	2
128167.85	tw[a]	R(1)	16p1	2	128160.60	P(1)	16pσ	2
128790.73	**128791.0**	R(1)	8pσ	3				
129365.19	**129367.1**	R(1)	9pπ	3	129281.00	P(1)	4pσ	8
129841.77	**129841.8**	R(1)	11p3	3	129822.20			
129962.38	129965.0[c]	R(1)	14p1	3	129969.20	P(1)	14pσ	3
130300.92	130301.4[d]	R(1)	21p1	3	130296.70	Q(1)	21pπ	3
130318.83	**130318.1**	R(1)	22p1	3	130311.60	P(1)	22pσ	3
130357.63	tw[a]	R(1)	16p3	3	130355.00	Q(1)	24pπ	3
130392.49	130392.0[e]	R(1)	27p1	3	130388.00	R(0)	22p0	3
130400.36	130400.5[f]	R(1)	17p3	3	130392.00	R(1)	27p1	3
130407.35	tw[a]	R(1)	28p1	3	130400.50	R(1)	17p3	3

[a]tw: too weak to be detected.
[b]Reference 9.
[c]Coincides with the R(0) 5pπ $v = 5$ line.[6]
[d]Coincides with the R(0) 7pπ $v = 4$ line.[6]
[e]Coincides with the R(1) 27p1 $v = 3$ line.[6]
[f]Coincides with the R(1) 17p3 $v = 3$ line.[6]

component may be dominant for the whole series of resonances: in such a case, the assignment was given to the resonance where it appears with a maximum component; the other resonances receive then the name of the second important component and so on. The last criteria used were that all the names of the levels involved in the mixing have to appear. We restricted our study to the np levels with $n > 7$ for which the dissociation continua do not cause instabilities in the calculations of the energies. For the intensities, we chose conditions where the quasi discrete states of the continuum are not in quasi coincidence with the level under consideration.

The absorption spectrum together with the ionization and dissociation excitation spectra were recorded from 81 to 74 nm with a spectral resolution of 0.001 nm and a precision of the wavelength measurement of about 0.0006 nm (or 1 cm^{-1} in energy). These spectra allow absolute intensity measurements and therefore have absolute cross section scales. All the lines corresponding to the np Rydberg states with $v > 0$ are seen in the ionization excitation spectrum but neither in the fluorescence nor in the dissociation channels; their ionization yield was thus considered as 1. The measurements of the line positions and the line intensities were performed using the ionization excitation spectra because this spectrum is far less noisy than the absorption one and enables further differentiation: some lines blended in the absorption spectrum may appear isolated in the ionization excitation spectrum.

The complete lists of levels, including the energies (calculated and observed) and the R and P line intensities (calculated and observed), are available separately via the supplementary material.[37]

A. Level energies

The energies of the $N = 2$ ortho singlet np levels of H_2 converging to the first four vibrational levels of H_2^+ have been measured earlier with very high precision (0.3 cm^{-1}) by Herzberg and Jungen.[6] These measurements are used as reference to test the quality of the calculations. The histogram of the discrepancies is shown in Figure 1(a). It can be fitted by a Gaussian centered at 0.07 cm^{-1} ($\pm$0.01) with a width of 0.53 cm^{-1} ($\pm$0.02). The precision of the calculations does not deteriorate due to the increase of the Coriolis coupling.[5] Obviously for several lines the deviations are far outside the Gaussian. The following discussion of the discrepancies, based on the new energy calculations, will lead to a number of reassignments of the former line energies.[6] The results are gathered in Table I for the $v = 0$ to $v = 3$ series and in Table II for $v = 4$ to $v = 6$.

- In the $v = 0$ Rydberg series, two lines are concerned: first, the R(1) 16p3 line calculated at 124211.53 cm^{-1} and measured at 124211.8 cm^{-1}. The formerly measured[6] value of 124215.70 cm^{-1} corresponds

TABLE II. Calculated $J = 2$ level energies and R(1) and P(3) line intensities ($v - v'' = 0$) for the $v = 4$ to 6 np1 and np3 levels. 4th, 10th, and 16th columns: o-c, observed–calculated energy values (both present work). The intensity values for the 8p3 $v = 4$ lines are integrated values over the mega-resonance (bold characters).

				A (10^6 s^{-1})						A (10^6 s^{-1})						A(10^6 s^{-1})	
	Level energy		o-c	R(1)	P(3)		Level energy		o-c	R(1)	P(3)		Level energy		o-c	R(1)	P(3)
8p1	4	130709.98	− 0.1	0.338	0.031	8p1	5	132341.83	− 0.4	0.070	0.006	8p1	6	133907.20	− 0.1	0.338	0.260
8p3	4	130884.70	− 0.2	**1.345**	**0.004**	8p3	5	132641.23		0.119	0.534	8p3	6	134139.25		0.031	0.000
9p1	4	131122.99	0.3	3.486	0.001	9p1	5	132813.23	2.4	2.478	0.107	9p1	6	134405.53		0.529	0.545
9p3	4	131276.97	0.9	1.159	0.717	9p3	5	132961.34	− 0.6	0.047	2.657	9p3	6	134516.66	1.8	0.042	0.865
10p1	4	131400.16	− 0.8	0.885	0.224	10p1	5	133097.66	− 0.9	0.731	0.288	10p1	6	134689.49	− 1.0	0.688	0.021
10p3	4	131523.86	1.9	0.302	1.029	10p3	5	133193.49		0.094	2.861	11p1	6	134808.81		0.478	0.641
11p1	4	131603.76	− 1.6	1.696	1.482	11p1	5	133295.91	− 1.0	0.706	0.059	10p3	6	134888.06		0.257	0.345
12p1	4	131698.06	− 0.3	0.370	0.009	12p1	5	133411.20	2.7	1.088	0.155	12p1	6	134981.35		0.465	0.077
11p3	4	131750.55	− 2.2	0.519	0.023	11p3	5	133471.69	− 0.1	0.069	0.938	11p3	6	135044.47		0.040	0.383
13p1	4	131836.67	− 0.6	0.803	0.066	13p1	5	133534.54	0.6	0.622	0.036	13p1	6	135116.01	0.4	0.140	0.047
12p3	4	131907.18	0.8	1.189	0.706	14p1	5	133591.95	− 0.4	0.477	0.302	12p3	6	135160.01		0.000	0.081
14p1	4	131943.32		0.003	0.988	12p3	5	133638.21		0.080	0.288	14p1	6	135221.98		0.164	0.076
13p3	4	131991.25	− 0.5	0.719	0.005	15p1	5	133689.68	1.3	0.145	0.029	15p1	6	135264.72		0.082	0.213
15p1	4	132031.79	2.7	0.480	0.248	13p3	5	133724.54		0.000	0.414	13p3	6	135300.35		0.010	0.235
16p1	4	132062.55	− 0.9	0.072	0.274	16p1	5	133760.82	− 0.3	0.166	0.133	16p1	6	135345.09		0.116	0.042
17p1	4	132102.05		0.026	0.191	17p1	5	133795.28	2.3	0.120	0.027	17p1	6	135364.80		0.006	0.057
18p1	4	132130.38		0.041	0.751	14p3	5	133820.25		0.001	0.700	14p3	6	135400.22	− 1.5	0.284	0.026
14p3	4	132150.34	− 1.1	0.083	0.337	18p1	5	133848.93	− 0.4	0.150	0.070	18p1	6	135432.20		0.000	0.120
19p1	4	132176.98	0.1	0.193	0.000	19p1	5	133873.51	0.4	0.069	0.005	15p3	6	135440.71	− 3.1	0.614	0.029
20p1	4	132199.71		0.089	0.267	15p3	5	133891.97		0.023	0.105	19p1	6	135469.82	− 0.4	0.686	0.017
15p3	4	132215.80		0.013	0.287	20p1	5	133913.61	− 0.6	0.110	0.069	20p1	6	135498.97		0.150	0.022
21p1	4	132234.27	− 0.4	0.121	0.040	21p1	5	133932.99		0.059	0.011	21p1	6	135520.08	1.0	0.598	0.026
22p1	4	132252.41	0.2	0.132	0.026	22p1	5	133945.99		0.024	0.018	22p1	6	135535.21	1.4	0.403	0.133
23p1	4	132266.31		0.019	0.257	16p3	5	133961.58		0.130	0.037	16p3	6	135548.68		0.001	0.080
16p3	4	132278.49		0.034	0.198	23p1	5	133978.02	− 0.1	0.105	0.032	23p1	6	135563.25		0.031	0.105
24p1	4	132292.00	0.0	0.095	0.032	24p1	5	133988.91		0.030	0.034	24p1	6	135574.61		0.127	0.129
25p1	4	132304.47	− 0.5	0.094	0.014	17p3	5	133996.79	− 0.5	0.297	0.001	17p3	6	135586.11		0.009	0.055
26p1	4	132314.28		0.021	0.194	25p1	5	134009.71	− 0.1	0.301	0.000	25p1	6	135598.27		0.018	0.035
17p3	4	132323.03		0.011	0.217	26p1	5	134021.88	0.0	0.432	0.022	26p1	6	135607.43	− 1.0	0.103	0.045
27p1	4	132332.63		0.050	0.091	27p1	5	134033.41	0.6	0.176	0.000	27p1	6	135613.77		0.019	0.009
28p1	4	132348.42		0.039	0.212	28p1	5	134043.19	0.4	0.241	0.009	28p1	6	135623.44		0.002	0.002
29p1	4	132352.88		0.008	0.315	29p1	5	134051.50	1.0	0.268	0.054	29p1	6	135633.15		0.013	0.005
30p1	4	132359.98		0.030	0.126	18p3	5	134057.69		0.122	0.125	18p3	6	135639.46		0.001	0.469
31p1	4	132366.76		0.020	0.067	30p1	5	134063.36		0.001	0.061	30p1	6	135642.19		0.027	0.002
32p1	4	132371.33		0.003	0.009	31p1	5	134069.81		0.055	0.011	31p1	6	135650.22		0.033	0.015
18p3	4	132375.44		0.041	0.010	32p1	5	134076.08	0.5	0.096	0.000	32p1	6	135657.41	0.6	0.039	0.048
19p3	4	132406.53		0.020	0.016	33p1	5	134081.73	1.4	0.109	0.008	33p1	6	135667.74		0.002	0.223
20p3	4	132434.51		0.011	0.009	34p1	5	134086.66	1.4	0.075	0.032	19p3	6	135672.19		0.013	0.047
21p3	4	132459.94		0.007	0.002	19p3	5	134091.09		0.017	0.046	34p1	6	135677.25		0.028	0.003
23p3	4	132504.65	− 0.9	1.163	0.127	20p3	5	134122.45		0.000	0.015	35p1	6	135682.12	− 0.1	0.031	0.002
24p3	4	132519.86		0.117	0.457	21p3	5	134151.37		0.001	0.003	36p1	6	135686.52	− 0.2	0.022	0.021
25p3	4	132534.66		0.026	0.159	23p3	5	134190.57	− 0.3	0.184	0.045	37p1	6	135690.31	0.6	0.001	0.061
26p3	4	132547.97		0.007	0.092	24p3	5	134206.87	− 1.1	0.221	0.000	38p1	6	135693.54		0.046	0.090
27p3	4	132559.88		0.002	0.062	25p3	5	134220.39	1.1	0.823	0.203	20p3	6	135696.40		0.376	0.072
28p3	4	132570.55		0.000	0.043	26p3	5	134238.55	2.1	0.459	0.673	39p1	6	135700.62		0.015	0.043
29p3	4	132580.13		0.000	0.030	27p3	5	134249.40	0.1	0.109	0.330	40p1	6	135703.67		0.008	0.025
30p3	4	132588.78		0.001	0.019	28p3	5	134259.74	− 1.5	0.039	0.213	41p1	6	135706.66		0.033	0.012

to the calculated P(1) 28pσ line. (The calculated value also coincides with the R(0) 23p0 line.) The second case is the 21p1 R(1) line calculated at 124108.58 cm^{-1} and measured at 124108.7 cm^{-1} as a small structure in the wing of the intensive R(0) 4pπ $v = 3$ line. The formerly measured[6] value of 124113.10 cm^{-1} is in coincidence with that R(0) 4pπ $v = 3$ line.

- In the $v = 1$ series, once again two R(1) lines are concerned: the 9pπ and the 24p1 ones. The R(1) 9pπ line calculated at 125416.24 cm^{-1} and measured at 125416.0 cm^{-1} is blended with the intensive R(0) 6pσ $v = 2$ line. The formerly measured[6] value of 125421.50 cm^{-1} corresponds to the latter R(0) line. The R(1) 24p1 line was calculated at 126354.58 cm^{-1}

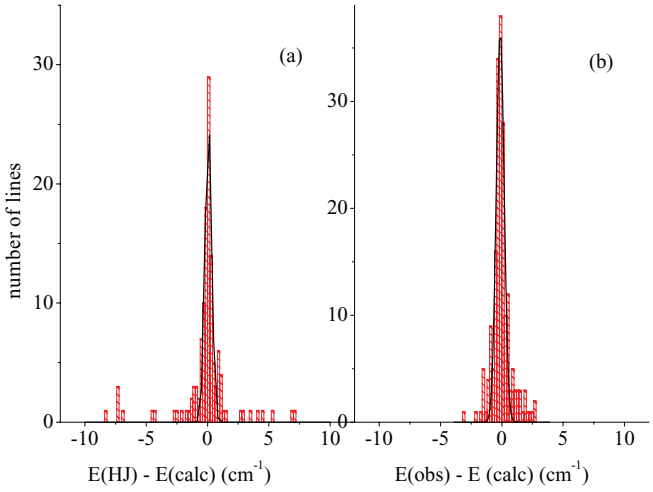

FIG. 1. Histogram representing the differences observed energy–calculated energy (MQDT fully *ab initio*): (a) for 128 *n*p Rydberg levels ($n > 7$) $v = 0$ to 3 of H_2 with observed values from Ref. 6. The full line represents its Gaussian fit with a maximum at $+0.07$ cm^{-1} and a full width of 0.53 cm^{-1}; many lines are found far out the Gaussian fit. (b) For 190 *n*p Rydberg $N = 2$ levels ($n > 7$) $v = 0$ to 6 of H_2, present work. The full line represents its Gaussian fit with a maximum at –0.13 cm^{-1} and a full width of 0.64 cm^{-1}. No lines are found with discrepancies higher than 3 cm^{-1}.

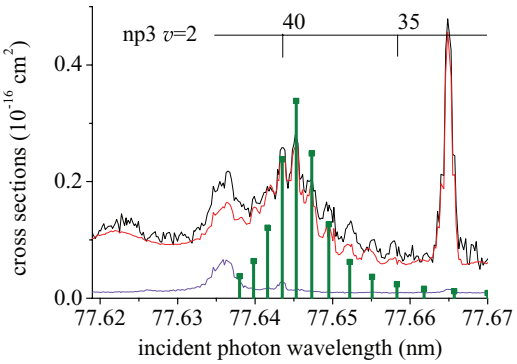

FIG. 2. A section of the excitation spectra of H_2 below the $v = 2$ ionization threshold showing a mega-resonance due to the 8pσ $v = 3$ level embedded in the *n*p3 $v = 2$ Rydberg series: (a) photoabsorption (black curve), (b) photoionization (red curve), (c) photodissociation (blue curve), (d) R(1) line cross sections calculated for a width equal to the apparatus function (green bars).

and agrees with the corresponding value measured by Dehmer *et al.*[9] and with that measured by Herzberg and Jungen[6] for the 23p0 R(0) line. The formerly measured[6] value of 126352.1 cm^{-1} agrees with the calculated value of the 24pσ P(1) line. There is better agreement here of our calculated values with Dehmer *et al.*'s results than with those of Herzberg and Jungen. Our calculated energies agree with the previous MQDT calculations of Ref. 19 within a few tenths of cm^{-1} although the present calculations used *ab initio* input data. (The R(1) 19p1 line also listed in Table I is too weak to be observed.)

- In the $v = 2$ series, there is disagreement for two R(1) lines: the 9pπ and the 16p1 ones. The calculated intensities of the 9pπ and 16p1 R(1) $v = 2$ lines are nearly zero and so the lines cannot be observed. It is similar for the 16p1 R(1) $v = 2$ line, The formerly measured[6] energy of the first one agrees with the calculated value for the P(1) 10pσ line The formerly measured[6] energy of the second one agrees with that of the 16pσ P(1) line whose calculated intensity is too low to be observed. O'Halloran *et al.*[8] reassigned this line at 128178.0 cm^{-1}, increasing the disagreement. Such a value has to correspond to a higher rotational level (J = 4). They also proposed to assign the 128304.9 cm^{-1} line to the R(1) 19p1 and the Q(1) line to 128307.3 cm^{-1}. The calculated values would lead to the reverse. The 17p1 R(1) and the Q(1) 17pπ lines have not been resolved in Herzberg and Jungen's spectrum but in the one of O'Halloran *et al.* who proposed the following assignments: 128231.2 cm^{-1} for the R(1) and 128229.8 for the Q(1) lines. The calculated values are, however, 128229.54 and 128231.17 cm^{-1} respectively, inverse to the proposal. For the 19p1 R(1) and 19pp Q(1) lines, the situation is the same: they proposed the R(1) line at 128304.9 cm^{-1} and the Q(1) line at 128307.3 cm^{-1}, the calculated values are 128307.47 and 128305.72, respectively. The calculated value of the 15p3 R(1) line agrees with the measured value of Ref. 8 whereas the measured value for the R(1) 25p1 line corresponds to the calculated value of the R(1) 16p3 line.
- In the $v = 3$ series, numerous lines are found in disagreement. In this spectral range, the absorption spectrum is clearly denser and the Rydberg series is much more perturbed. The R(1) 8pσ $v = 3$ line was observed at 128791.0 cm^{-1} and calculated as a mega resonance: the 8pσ $N = 2$ level is embedded in the quasi continuum of the *n*p3 $v = 2$ series, enhancing the line intensities of the nearby *n*p3 (from $n = 31$ to 41) R(1) lines (see Figure 2). In Ref. 6 the 9pπ line was assigned to the measured value of 129281.00 cm^{-1}. This position agrees, however, with the calculated one of the P(1) 4pσ $v = 8$ line. The 9pπ calculated position corresponds to a very broad structure visible also in the spectrum of Dehmer and Chupka.[7] The R(1) 11p3 line is quoted at 129822.20 cm^{-1} in Ref. 6. At this energy, no structure appears neither in Dehmer and Chupka's spectrum neither in ours; it may be a typing error: Its energy should read 129842.20 cm^{-1}. The R(1) 14p1 is calculated to be in superposition with the R(0) 5pπ $v = 5$ line. The formerly measured[6] energy of 129969.20 cm^{-1} corresponds to the calculated value of the P(1) 14pσ line. The R(1) 21p1 noted in coincidence with the Q(1) 21pπ line is calculated to be in coincidence with the R(0) 7pπ $v = 4$ line. The measured 22p1 R(1) position in Ref. 6 corresponds to the P(1) 22pσ line. The R(1) 16p3 line proposed as superposed to the Q(1) 24 pπ line is in fact too weak to be detected. The group of the 27p1, 17p3, and 28p1 lines receives an assignment shifted with respect to the previous[6] one: the 27p1 R(1) line calculated at 130392.49 cm^{-1}, at a position formerly assigned[6] to the 17p3 R(1) line, is found to be superposed to the R(0) 22p0 line. The 17p3 R(1) line calculated at 130400.36 cm^{-1} replaces the former

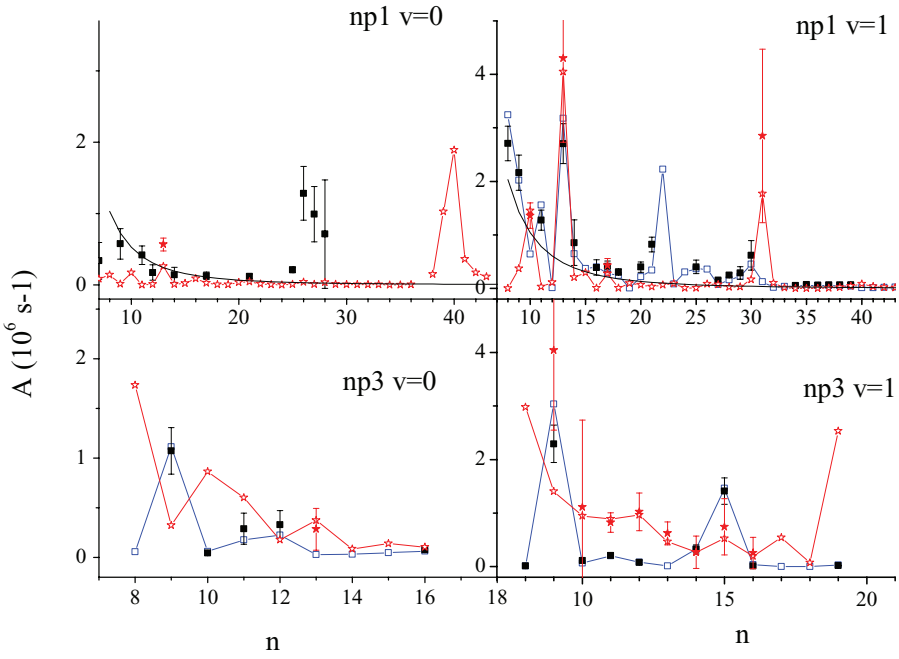

FIG. 3. Einstein A coefficients for the $np1$ levels (upper part) and $np3$ levels (lower part) for the $v = 0$ and 1 progressions. Black filled squares: experimental R(1) values; connected blue open squares: calculated values for R(1) lines; connected red open stars: calculated values for P(3) lines; red filled stars: experimental P(3) values.

assignment[6] as 28p1. The 28p1 line in turn is too weak to be detected. The new assignments are listed in Table I.

- For the $v = 4$ series, a full MQDT treatment has been published on a very small part of the spectrum including the 8pπ mega-resonance and the 9pσ resonance.[18] These calculations agree within a few tenths of cm^{-1} with ours although the present calculations are based on *ab initio* input data.
- For the $v = 0$ to 6 series, the calculated level energies were compared with the measured values obtained from our own spectra. The results of such a comparison made on 190 lines are displayed in a histogram in Figure 1(b). The distribution is somewhat broader than the distribution in Figure 1 since the precision obtained from a photographic plate is higher than that obtained from a scanning monochromator. The fitted Gaussian is peaked at -0.13 cm^{-1} showing that the calculations are pretty accurate, its width of 0.64 $\pm$ 0.03 cm^{-1} is nearly the same as in the case of Figure 1. The main difference is on the wings of the distribution, i.e., more lines present a shift of 1 to 2 cm^{-1}, all of them belonging to the higher vibrational series ($v = 4$ to 6) for which the density of the lines is extremely high; the mixings between the series are very strong. The precision of the calculations may be also a little smaller due to our approximation; at large internuclear distances, the configuration interactions may not be negligible any more. More than 140 calculated levels belonging to the $v = 4$ to 6 np series are listed for the first time, 65 of them were measured for the first time, even though a great number of them were visible in Figure 4 of Ref. 7. All these values are gathered in Table II.

B. Line intensities

We have calculated Einstein A coefficients corresponding to each observed line using the relation

$$\int \sigma d\lambda = \frac{\lambda^4}{8\pi c} A_{v',v'',N',N''} \frac{2N'+1}{2N''+1} n_{N''}$$

with $N' = N'' + 1$ for a R(N'') line and $N' = N'' - 1$ for a P(N'') line. Here σ is the measured absorption cross section which is integrated over the profile of a given line, and λ is the wavelength. n_N is the fraction of molecules in the rotational state $N'' = 1$ for the R(1) line or $N'' = 3$ for the P(3) line, (at room temperature $n_1 = 0.657$ and $n_3 = 0.092$). The fraction $(2N' + 1)/(2N'' + 1)$ is a degeneracy ratio arising from the choice of the emission A coefficient to describe an absorption process.

We measured the Einstein A coefficients for nearly 200 R(1) and P(3) lines belonging to the series $v = 0$ to 6 with $n > 7$ using Gaussian fits. For these Rydberg series, Hund's coupling case d is expected. In fact, we observed globally

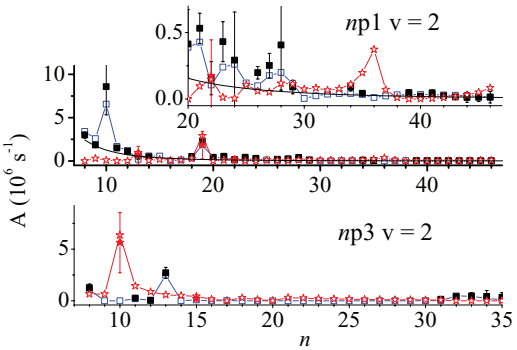

FIG. 4. Same as Figure 3 for the $v = 2$ vibrational progressions. In the inset: section corresponding to high n with enlarged ordinate scale.

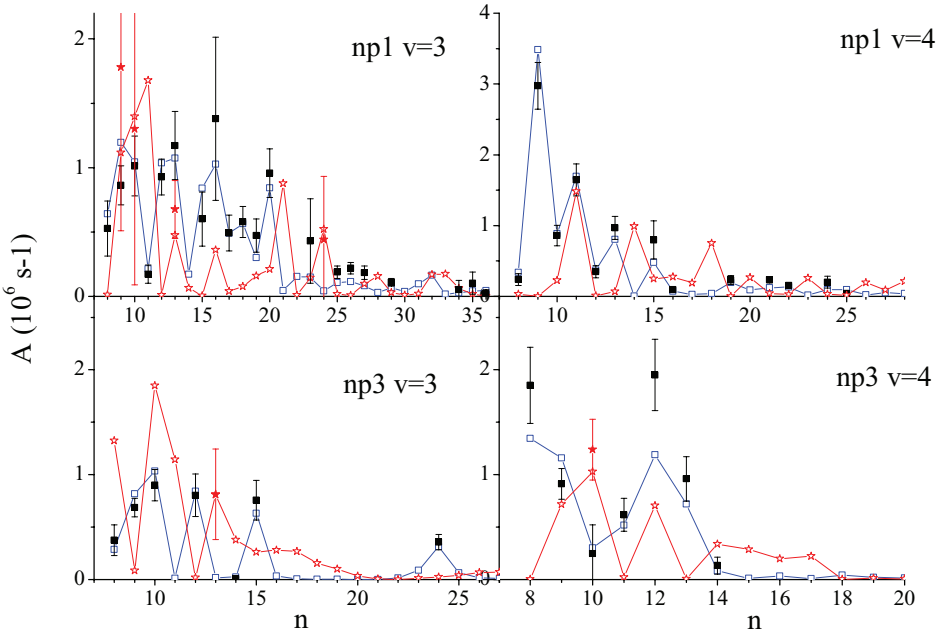

FIG. 5. Same as Figure 3 for the $v = 3$ and 4 vibrational progressions. The quoted intensities for the 9p3 $v = 4$ lines are summed up including the nearby 65p3 and 66p3 $v = 3$ lines which lie within the apparatus function.

that the *n*p1 levels are mainly excited through the R(1) lines, whereas the *n*p3 levels are mainly excited through the P(3) lines. This propensity rule exhibits many exceptions, as they are strongly perturbed (by each other and by levels of other series).

The uncertainties of the intensity measurements were estimated taking into account the statistics (3 standard deviations) and the uncertainty on the absolute calibration of the spectra (10%). The uncertainties of the intensity calculations may be estimated from the variations obtained by varying the conditions (number of channels, maximum internuclear distance, conditions of integration of the vibrational wave functions...). We cannot expect to get an uncertainty lower than 10%. Under these conditions, the agreement between the calculated and the measured intensity values is really good. The results are displayed in Figures 3–6 with the adiabatic calculated values of the R(1) *n*p1 lines extrapolated from the adiabatic values of the 5pσ R(1) $v' - v'' = 0$ lines scaled by the Rydberg $1/n^3$ law. The general tendency is fairly reproduced but the departures from these values may also be huge (multiplied by ~60 for the ~50p1 $v = 2$, for instance).

The intensities of the $v = 0$ *n*p1 R(1) series show three local strong perturbations, the first one between $n = 10$ and 14 by the 6pσ and 6pπ $v = 1$ levels, the second one for $n = 33$ to 35 by the 7pσ $v = 1$ level and the last one, not shown in Figure 3, for $n = 65$ to 75 by the 4pσ $v = 4$ level (inner well). In Hund's coupling case *d*, the A values of the *n*p1 P(3) lines vanish; the perturbations can mix the *n*p1 and *n*p3 series and enhance the intensities of the P(3) lines. This is what we can see for the $n = 10$ to 14 and 65 to 75 levels but not for the $n = 33$ to 35 ones, since the 7pσ level is almost 7p1 already. The 20p1 level is perturbed by the 4pπ $v = 3$ level and loses completely its *n*p1 character: it radiates mainly through the P line. These local perturbations by low Rydberg states have not been taken into account in the early QDT calculations[6] and that explains the reassignment of the two lines involved.

The $v = 1$ *n*p1 series shows again a perturbation for the low values of *n*, the 10p1 and 9p3 levels are located quite close to each other and interact strongly (see Figure 3). The 12p1 level interacts with the nearby 3pπ $v = 7$ and 6pπ $v = 2$ levels and loses its emission probability to them. On the contrary, the 13p1 level shares its emission probability with the 5pσ $v = 3$ one and both the R(1) and P(3) lines are greatly enhanced. The 22p1 level is located near the 7pσ $v = 2$ one and the mixing enhances the intensity of its R(1) line, as in the case of the $v = 0$ series. The 31p1 level is perturbed by the 5pπ $v = 3$ one and loses its *n*p1 character and radiates through the P(3) line mainly.

The $v = 2$ *n*p1 series (see Figure 4) is perturbed for $n = 10$ by the 5pσ $v = 4$ level, for $n = 19$ by the 4pσ $v = 7$ (inner-well) level, and for $n = 28$ to 30 by the 7pπ $v = 3$ level inducing the enhancement of the P line. The *n*p3 series is perturbed for $n = 10$ by the 6pπ $v = 3$ level enhancing the P line, for $n = 13$ by the 5pπ $v = 4$ and for $n = 35$–45 by the 8p1 $v = 3$ level resulting in a mega-resonance (see Figure 2).

For the $v = 3$ series, there are too many terms perturbed by low Rydberg members to be described in detail. Figure 5 illustrates the chaotic behavior of the intensities. That explains the extreme difficulties formerly encountered in the process of assigning the observed lines: There are in fact no regularities neither in the line intensities nor in the positions. Precise non-adiabatic calculations are essential for reliable assignments of this series.

For the $v = 4$ series, the situation is quite similar to that of the $v = 3$ one with a very strong perturbation for the

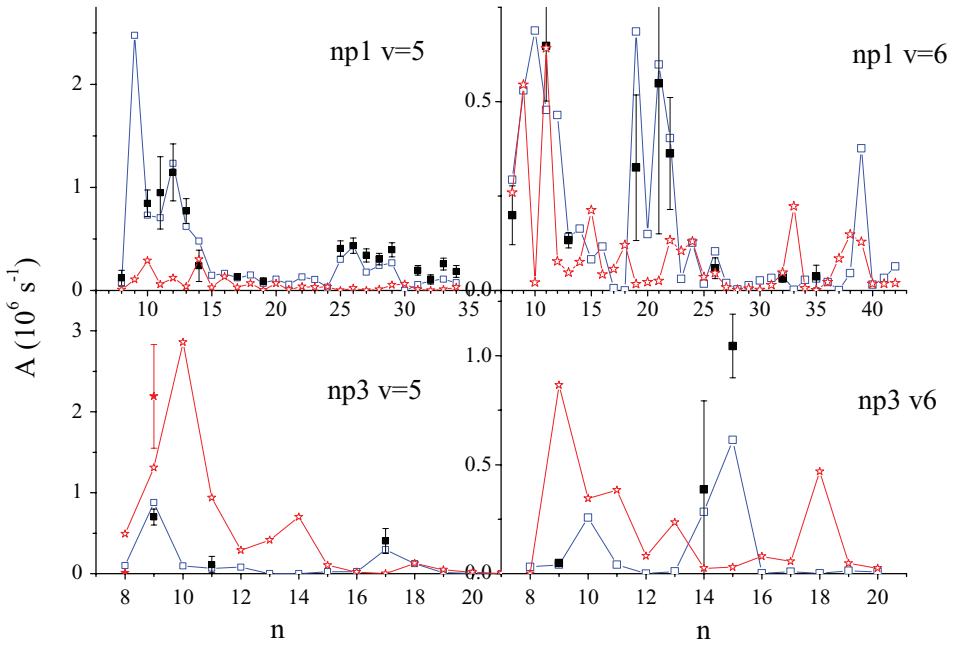

FIG. 6. Same as Figure 3 for the $v = 5$ and 6 vibrational progressions.

23p3 level which lies by less than 10 cm^{-1} higher than the 6pσ $v = 6$ level (Figure 5).

For the $v = 5$ series, the first members are perturbed as for the other series (Figure 6); for the higher values, we can see a mega-resonance at the 25-30p1 levels due to the mixing with the 8p1 $v = 6$ level. A second mega-resonance appears at the 23–27p3 levels due to the 5pσ $v = 10$ resonance. At such an energy, located above the $H(1s) + H(n = 3)$ threshold, the 5pσ state presents a shape resonance (the $v = 10$ level) due to a potential barrier located at 5.7a_0. This shape resonance appears in the MQDT calculations as a discrete state in interaction with the Rydberg np3 $v = 5$ series, spreading the absorption intensity on several Rydberg lines. A third mega-resonance appears at the 40–50 p3 levels due to the 6pπ $v = 7$ level. In this case, the energy gap between two consecutive lines is smaller than the apparatus function and we see only one broad structure in the spectrum (see Figure 7).

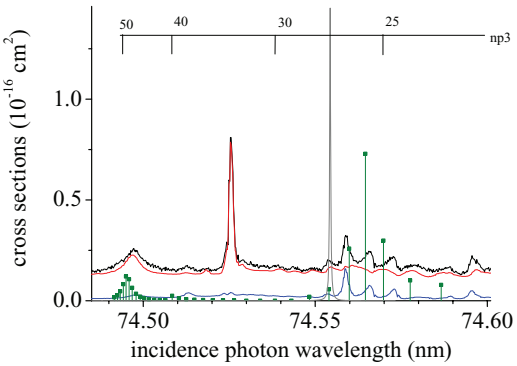

FIG. 7. Same as Figure 1, showing two mega-resonances in the np3 $v = 5$ progression. The first one around $n = 26$ is due to the proximity of the 5pσ $v = 10$ resonance; the adiabatic calculations of the dissociation cross section of the 5pσ is also displayed (grey curve): it shows that the non-adiabatic couplings shift and spread the resonance. The second mega-resonance around $n = 48$ is due to the nearby 6pπ $v = 7$ level.

The $v = 6$ series, similar to the previous ones, presents many irregularities. In the np1 series, for $n = 19$–23, a mixing occurs with the 8p1 $v = 7$ and the 4pπ $v = 11$ levels and the 33p1 level is mixed with the 8p3 $v = 7$ one enhancing the P line. The measurements become more and more difficult as the intensities decrease and the density of the lines increases.

From the calculations and from the measurements, we can conclude the systematical observation that the intensities of R(1) lines of a np v Rydberg series are enhanced by the perturbation of a npσ lower Rydberg level and the P(3) lines by the perturbation of a npπ level, respectively, in accordance with the Hund's coupling case *d*.

V. CONCLUSION

As we did before for the R(0) lines,[5] we calculated systematically by a full *ab initio* MQDT treatment the energies and intensities of around 500 R(1) lines and 500 P(3) lines corresponding to the np1 and np3 $v = 0$ to 6 Rydberg series (for $n > 7$). In these calculations, we assumed that the manifold of the $^1\prod_u$ and $^1\sum_u^+$ states of H_2 represents a single np Rydberg series converging to the X $^2\sum_g^+$ state of the ion, disregarding configuration interactions (nf Rydberg series and np doubly excited core).

We compared these values with the experimental values of Herzberg and Jungen[6] for the $v = 0$ to 3 series. Apart from a few number of reassignments needed, the calculated and experimental energies agree within 1 cm^{-1} or less, showing that our single-configuration approach is adequate for these Rydberg states; the mixings with the 1s-nf states or with the doubly excited 2sσ-np ones are negligible. The earlier analysis[6] was based on a QDT analysis (the npσ-npπ coupling) extended by the vibrational interaction between $\Delta v = 1$ levels. The present treatment includes all the possible couplings between all the levels of 1s, np configuration, i.e., between np

and n'p, and for all possible values of Δv. Therefore, it represents a clear improvement in analysing the spectrum and made several reassignments necessary.

We measured the energies and the intensities of nearly 200 R(1) lines and around 70 P(3) lines. All the intensity measurements were done for the first time. Sixty nine R(1) lines belonging to the $v = 4$ to 6 vibrational series were assigned for the first time, extending the assigned spectrum by more than 4000 cm^{-1}. For all these lines, the MQDT calculations reproduced their energies and their intensities. We observed that for the series with the highest v measured ($v = 6$) the agreement between observed and calculated values deteriorates a bit, from 1 cm^{-1} to 2 or 3 cm^{-1}. This may be due to the increasing importance of configuration interactions at large internuclear distances.

In order to calculate the H_2 absorption spectrum completely (at low temperature), we need to solve the problem of the low Rydberg levels sensitive to the dissociation. A unified treatment of dissociation and ionization processes in H_2 has already been developed successfully (see Refs. 16 and 38). Moreover, the $B''\overline{B}$ state is a double-well state: at short internuclear distance, it is the third $np\sigma$ Rydberg state of the fundamental state X of the ion, and at large distance, it becomes the first $2p\sigma$ Rydberg state of the first excited $2s\sigma$ state of the ion. In order to reproduce its spectrum above the potential barrier, we need to take into account the doubly excited states of the ion; this problem was solved for the $^1\sum_g^+$ states of H_2 in a non-*ab initio* approach.[39–41]

This study is another step further ahead toward our goal of the full theoretical *ab initio* analysis of the observed absorption spectrum of H_2 at room temperature up to the $H(n = 4 \text{ (or } 5)) + H(n = 1)$ dissociation limit.

ACKNOWLEDGMENTS

We acknowledge the Helmholtz-Zentrum Berlin – Electron storage ring BESSY II for providing synchrotron radiation at beamline U125/2-10m-NIM and we would like to thank Gerd Reichardt and Andreas Balzer for their assistance. The research leading to these results has received funding from the European Community's Seventh Framework Programme (FP7/2007-2013) under Grant Agreement No. 226716. AK would likes to thank the Otto-Braun-Fonds of the University of Kassel for financial support.

[1]M. Glass-Maujean and Ch. Jungen, J. Phys. Chem. A **113**(47), 13124 (2009).
[2]M. Glass-Maujean, Ch. Jungen, and H. Schmoranzer *et al.*, Phys. Rev. Lett. **104**(18), 183002 (2010).
[3]M. Glass-Maujean, Ch. Jungen, and G. Reichardt *et al.*, Phys. Rev. A **82**(6), 062511 (2010).
[4]M. Glass-Maujean, C. Jungen, and H. Schmoranzer *et al.*, J. Chem. Phys. **135**(14), 144302 (2011).
[5]M. Glass-Maujean, H. Schmoranzer, and I. Haar *et al.*, J. Chem. Phys. **136**(13), 134301 (2012).
[6]G. Herzberg and Ch. Jungen, J. Mol. Spectrosc. **41**, 425 (1972).
[7]P. M. Dehmer and W. A. Chupka, J. Chem. Phys. **65**, 2243 (1976).
[8]M. A. O'Halloran, P. M. Dehmer, and F. S. Tomkins *et al.*, J. Chem. Phys. **89**, 75 (1988).
[9]J. L. Dehmer, P. M. Dehmer, and S. T. Pratt *et al.*, J. Chem. Phys. **90**(11), 6243 (1989).
[10]L. Wolniewicz, T. Orlikowski, and G. Staszewska, J. Mol. Spectrosc. **238**(1), 118 (2006).
[11]U. Fano, Phys. Rev. A **2**(2), 353 (1970).
[12]Ch. Jungen and O. Atabek, J. Chem. Phys. **66**, 5584 (1977).
[13]Ch. Jungen and D. Dill, J. Chem. Phys. **73**, 3338 (1980).
[14]M. Raoult, Ch. Jungen, and D. Dill, J. Chim. Phys. (Paris) **77**(7/8), 599 (1980).
[15]M. Raoult and Ch. Jungen, J. Chem. Phys. **74**, 3388 (1981).
[16]Ch. Jungen, Phys. Rev. Lett. **53**, 2394 (1984).
[17]C. H. Greene and Ch. Jungen, Adv. At. Mol. Phys. **21**, 51 (1985).
[18]J. A. Stephens and C. H. Greene, J. Chem. Phys. **100**, 7135 (1994).
[19]Ch. Jungen, S. T. Pratt, and S. C. Ross, J. Phys. Chem. **99**, 1700 (1995).
[20]Ch. Jungen, *Molecular Applications of Quantum Defect Theory* (Institute of Physics, Bristol, 1996).
[21]G. Staszewska and L. Wolniewicz, J. Mol. Spectrosc. **212**(2), 208 (2002).
[22]L. Wolniewicz and G. Staszewska, J. Mol. Spectrosc. **220**(1), 45 (2003).
[23]M. Glass-Maujean, S. Klumpp, and L. Werner *et al.*, J. Chem. Phys. **126**(14), 144303 (2007).
[24]M. Glass-Maujean, S. Klumpp, and L. Werner *et al.*, Mol. Phys. **105**(11–12), 1535 (2007).
[25]A. Glass-Maujean, S. Klumpp, and L. Werner *et al.*, J. Mol. Spectrosc. **249**(1), 51 (2008).
[26]M. Glass-Maujean, S. Klumpp, and L. Werner *et al.*, J. Chem. Phys. **128**(9), 094312 (2008).
[27]G. Reichardt, J. Bahrdt, J.-S. Schmidt *et al.*, Nucl. Instrum. Methods Phys. Res. A **462**, 467 (2001).
[28]L. Wolniewicz and G. Staszewska, J. Mol. Spectrosc. **217**(2), 181 (2003).
[29]J. Vigué, J. A. Beswick, and M. Broyer, J. Phys. (Paris) **44**, 1225 (1983).
[30]M. Glass-Maujean, P. Quadrelli, and K. Dressler, J. Chem. Phys. **80**, 4355 (1984).
[31]M. Glass-Maujean and J. A. Beswick, J. Chem. Soc., Faraday Trans. 2 **85**, 983 (1989).
[32]H. Wind, J. Chem. Phys. **42**, 2371 (1965).
[33]D. M. Bishop and R. W. Wetmore, Mol. Phys. **27**, 279 (1974).
[34]L. Wolniewicz and T. Orlikowski, Mol. Phys. **74**, 103 (1991).
[35]L. Wolniewicz, J. Chem. Phys. **99**(3), 1851 (1993).
[36]J. Liu, E. J. Salumbides, and U. Hollenstein *et al.*, J. Chem. Phys. **130**, 174306 (2009).
[37]See supplementary material at http://dx.doi.org/10.1063/1.4742311 for the level list with energies and line intensities.
[38]Ch. Jungen and S. Ross, Phys. Rev. A **55**, R2503 (1997).
[39]S. Ross and Ch. Jungen, Phys. Rev. Lett. **59**, 1297 (1987).
[40]S. Ross and C Jungen, Phys. Rev. A **49**, 4353 (1994).
[41]S. Ross and C Jungen, Phys. Rev. A **49**, 4364 (1994).